Control of Perfusable Microvascular Network Morphology Using a Multiculture Microfluidic System

Jordan A. Whisler, MS,[1] Michelle B. Chen, BS,[1] and Roger D. Kamm, PhD[1,2]

The mechanical and biochemical microenvironment influences the morphological characteristics of microvascular networks (MVNs) formed by endothelial cells (ECs) undergoing the process of vasculogenesis. The objective of this study was to quantify the role of individual factors in determining key network parameters in an effort to construct a set of design principles for engineering vascular networks with prescribed morphologies. To achieve this goal, we developed a multiculture microfluidic platform enabling precise control over paracrine signaling, cell-seeding densities, and hydrogel mechanical properties. Human umbilical vein endothelial cells (HUVECs) were seeded in fibrin gels and cultured alongside human lung fibroblasts (HLFs). The engineered vessels formed in our device contained patent, perfusable lumens. Communication between the two cell types was found to be critical in avoiding network regression and maintaining stable morphology beyond 4 days. The number of branches, average branch length, percent vascularized area, and average vessel diameter were found to depend uniquely on several input parameters. Importantly, multiple inputs were found to control any given output network parameter. For example, the vessel diameter can be decreased either by applying angiogenic growth factors—vascular endothelial growth factor (VEGF) and sphingosine-1-phsophate (S1P)—or by increasing the fibrinogen concentration in the hydrogel. These findings introduce control into the design of MVNs with specified morphological properties for tissue-specific engineering applications.

Introduction

Engineered biological tissue for implantation and regenerative therapies requires a functional microvasculature to ensure proper function and survival in its intended working environment. It is likely that the desired microvascular network (MVN) morphology of an engineered tissue will vary depending on its ultimate function in the body. This can be inferred from the significant differences found in the microvasculature of various organs *in vivo* and across species.[1] For instance, islet cells cannot survive separation distances from the nearest capillary greater than 0.1 mm due to insufficient diffusion of oxygen, whereas chondrocytes in cartilage tissue can survive distances exceeding 1 mm.[2] By controlling the diameter of engineered microvessels and the branching characteristics of their networks, the optimal perfusion rate and separation distance for a specific tissue can be achieved. Along these lines, Hoganson *et al.*[3] applied a biomimetic design approach to the tissue-specific microvascular requirements of the liver to reproduce physiological blood flow characteristic for that organ. Additionally, many mathematical models—originating with the theory set forth by Murray,[4] based on the principle of minimum work—have been developed to determine the optimal design of a MVN.[1,5–7] However, these designs have generally been im-

plemented in the form of preformed vascular molds, which are subsequently seeded with endothelial cells (ECs)[8] and thus do not mimic the complex process of vascular network formation *in vivo*. There has been remarkable progress recently in forming perfusable MVNs in three-dimensional hydrogels without the need for artificial architecture to support the vascular structures.[9–12] Still lacking, however, is a systematic study of the factors controlling the network morphology and the effects of signaling between different cell types.

Moreover, the dominating influence determining network morphology is generally assumed to consist of fluid flow dynamics and related shear forces acting on the endothelium. However, it has long been recognized that mechanical and biochemical properties of the microenvironment can also play important roles in determining MVN morphology. The goal of our research was, therefore, to probe the biochemical and mechanical environment of ECs undergoing the process of vasculogenesis in a three-dimensional hydrogel to determine the influence of these factors on the morphological characteristics of the resulting engineered MVNs. By uncovering these design principles, we are able to take advantage of the natural control mechanisms employed *in vivo* to guide MVN formation toward a desired morphology.

Departments of [1]Mechanical Engineering and [2]Biological Engineering, Massachusetts Institute of Technology, Cambridge, Massachusetts.

To achieve this goal, we used a multiculture perfusable microfluidic platform enabling real-time observation and independent control over paracrine signaling, cell-seeding densities, and hydrogel mechanical properties (Fig. 1A, B). Human umbilical vein endothelial cells (HUVECs) were seeded in fibrin gels and cultured alongside—but not in contact with—human lung fibroblasts (HLFs). HUVECs spontaneously formed networks within 24 h and the engineered vessels contained patent, perfusable lumens as demonstrated by the passage of fluorescent microspheres
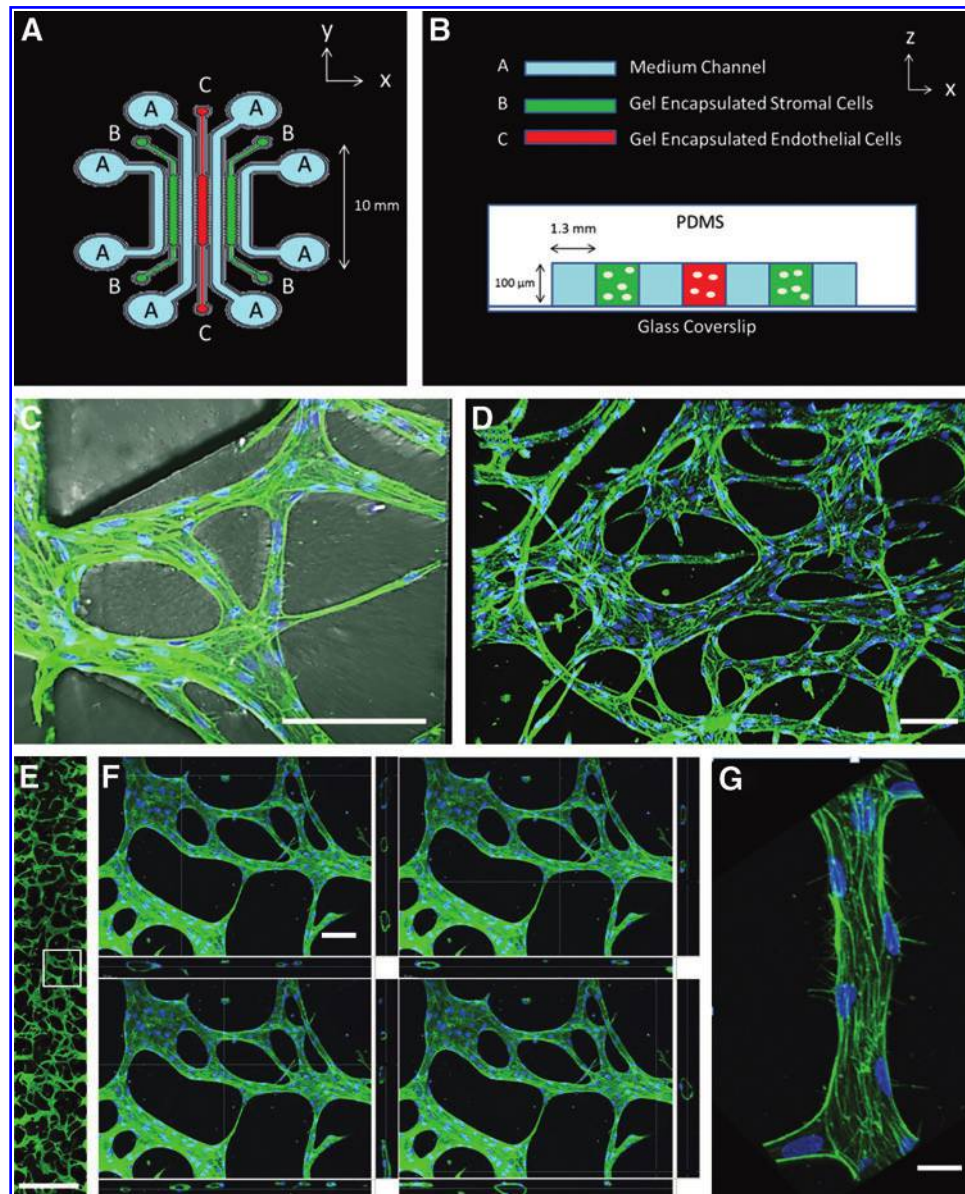
FIG. 1. **(A)** Top view diagram of multiculture microfluidic device containing three parallel gel regions for encapsulation of endothelial and stromal cells. Gel regions (B, C) are separated by medium channels (A) for gas exchange and delivery of nutrients. **(B)** A cross-sectional view diagram of multiculture microfluidic device. Cell culture region is surrounded by PDMS above and glass coverslip below (not to scale). **(C)** Top view of perfusable vessels opening to medium channel on left. Region shown is between two PDMS trapezoidal posts. Twenty such regions exist in each microfluidic device. Staining: Green–phalloidin; Blue–DAPI (same for **D–G**). Scale bar = 100 μm. **(D)** A 10× confocal image of perfusable microvascular network (MVN) grown in a multiculture microfluidic device. Scale bar = 100 μm. **(E)** Full image of vascularized gel region. White box corresponds to enlarged image in **(F)**. Scale bar = 1 mm. **(F)** Sequence of four section views taken throughout 20× confocal stack. Vertical cross sections on the bottom and right correspond to the location of the white crosshairs. As the cross sections progress through the vascularized region, patent lumens are seen to vary in location and diameter, but remain continuous throughout the gel. This demonstrates the existence of perfusable vessels spanning the 100 μm height of the gel region. Further validation of perfusability is provided in the Supplementary videos. Scale bar = 100 μm. **(G)** A 40× confocal image of a segment of perfusable microvessel showing multiple cells. Scale bar = 10 μm. See Supplementary video SV1 for three-dimensional rendering with visualization of lumen. Color images available online at www.liebertpub.com/tec

after 4 days (Supplementary Videos SV2 and SV3; Supplementary Data are available online at www.liebertpub.com/tec). Communication between the two cell types was necessary to avoid network regression and maintain stable morphology beyond 4 days. Fluorescent imaging and subsequent analysis were used to quantify the number of branches, average branch length, percent vascularized area, and average vessel diameter of the MVNs generated under various conditions. Finally, results were tabulated and the design parameter space was mapped out for the conditions studied.

This study provides quantitative results for direct use in the design of engineered MVNs. It also demonstrates the powerful capabilities of miniaturized, perfusable, three-dimensional engineered MVNs to study the influence of a multitude of environmental cues affecting network morphology in a high-throughput and readily observable manner. It more generally demonstrates the ability to approach microvascular tissue engineering as a design problem using systematic, quantitative analysis.

Materials and Methods

Device design and fabrication

A standard procedure for generating silicone molds was used.[13] Briefly, computer aided designs (CAD) were generated and used to print negative pattern transparency masks. A 100 μm layer of SU-8 photoresist was coated onto a silicon wafer, and the mask was used to photopolymerize the pattern on to the wafer.

The mask was repeatedly used to form microfluidic chips. Briefly, PDMS (Ellsworth Adhesives) and a curing agent were mixed at a 10:1 ratio and poured onto the wafer. After degassing, the PDMS was baked in an 80°C oven for 2 h. The individual devices were then cut out and a biopsy punch was used to create ports for gel filling and medium channels. Tape was used to remove dust from the surface, and the devices were placed in an autoclave for sterilization. Clean devices and coverslips were plasma treated (Harrick Plasma) and bonded together.

The design of this multiculture vasculogenesis device was based on earlier designs from our laboratory[14] with some important adjustments: (1) a third parallel gel region was included so that stromal cells could be cultured on either side of the vascularized gel region, (2) additional medium channels were included so that each gel region is flanked by two medium channels—one on each side—to provide adequate gas exchange and supply of nutrients, and (3) the length of the device was increased to provide a larger region for vascularization.

The width of each gel and medium channel was chosen to be 1.3 mm. This was to ensure that the vascularized region's maximum dimension was at least 1 mm, such that diffusion is insufficient for delivering nutrients and removing wastes from the inner core of a living tissue. This is the length scale for which prevascularization is necessary.[15] The width as well as the length of the gel region could be increased to provide a larger vascularized area without affecting the dynamics of the system. Since the ECs and HLFs communicate through diffusive transport of secreted factors, the width of the medium channel determines the time scale for this process to occur. For typical growth factors, the time constant for

diffusion over a length of 1 mm is on the order of several hours. Since the process of network formation studied in our system occurs over a period of days, this width is sufficiently small to ensure adequate time for diffusion to occur. Because the necessary time for diffusion scales with the square of the distance between the gel regions, the width of the medium channel should not be increased. Finally, the dimensions of the fibroblast gel region, in combination with cell seeding density, determine the rate of secretion of growth factors and cytokines. We chose dimensions that enabled us to screen for the optimal seeding ratio between HUVECs and NHLFs within a range of 1:2–2:1 that is physiologically relevant and reported in other *in vitro* studies[16,17] (Results discussed below).

To achieve optimal imaging conditions, we chose a height of 100 μm for the device and sealed it with a glass coverslip. This height enabled us to form generally planar perfusable networks, allowing us to capture the MVN morphological patterns from a single focal plane using epifluorescence. The height could be increased for clinical applications, in which it might be desirable to form vascularized tissue constructs containing several planes of vessels.

Cell culture

HUVECs (Lonza) were cultured on collagen I-coated flasks (50 μg/mL collagen solution in ascetic acid for 30 min; BD Biosciences) in EGM-2 MV (Lonza) growth medium and used in experiments between passages 6–8. Normal human lung fibroblasts (NHLF; Lonza) were cultured in FBM-2 (Lonza) growth medium and used in experiments between passages 6–10.

For exogenous growth factor experiments, EGM-2 MV growth medium was supplemented with 50 ng/mL VEGF (Peprotech) and 250 nM S1P (Sigma). The medium was replenished every 2 days.

Fibrin gel cell encapsulation

Fibrinogen (Sigma) was dissolved in PBS (Lonza) at twice the final concentration (2.5–20 mg/mL for fibrin concentration experiments). Thrombin (Sigma) was dissolved in PBS at 2 U/mL. These solutions were mixed, over ice, at a 1:1 ratio to produce a final fibrinogen solution with the desired concentration (1.25–10 mg/mL). The mixture was quickly pipetted into the device using the gel filling ports. The device was placed in a humidified enclosure and allowed to polymerize at room temperature for 10 min before fresh growth medium was introduced to the medium channels. The growth medium was replaced every 2 days.

For gels with encapsulated cells, a similar procedure was followed. Cells were spun down at 1200 rpm for 5 min and the cell pellet was resuspended in EGM-2 MV growth medium containing 2 U/mL of thrombin and mixed with the fibrinogen solution at a 1:1 ratio. The device was placed in a humidified enclosure and allowed to polymerize at room temperature for 10 min before fresh growth medium was introduced to the medium channels.

Staining/imaging

After 4 days, cells in devices were fixed with 4% paraformaldehyde (Electron Microscopy Sciences) for 15 min and

rinsed 3×with PBS. Triton X (0.1%; Sigma) was then introduced to permeabilize the cells and rinsed 3×with PBS after 15 min. The devices were then treated with DAPI and phalloidin (Life Technologies) for 2 h to stain the nuclei and actin, respectively. Phalloidin staining was used to image vascular network morphology with an epifluorescent microscope (Nikon Eclipse Ti-S; Nikon Instruments, Inc.). Confocal images were taken with an Olympus IX81 microscope (Olympus America, Inc.).

Analysis/quantification

The procedure used to process and analyze fluorescent images is described in detail elsewhere.[18] Briefly, raw images were prepared by enhancing contrast and removing noise. Automatic thresholding was used to binarize the images. Unconnected segments, which were not part of the perfusable networks, were automatically removed from the images. Finally, networks were skeletonized and analyzed[19] using ImageJ software (http://rsbweb.nih.gov/ij/).

Effective diameter calculations were performed by dividing the thresholded vascularized area by the entire length of the skeletonized network.

For perfusability experiments with fibroblasts, the regions between PDMS posts containing vessels opening to the adjacent medium channels were counted and expressed as a percentage of the total number of regions.

Bead flow experiments

For bead flow experiments, vascular networks were fixed and stained as described above. Ten micrometer fluorescent microspheres (Life Technologies) were perfused through the networks by imposing a hydrostatic pressure drop across the EC gel region. Videos were recorded using NIS-Elements software (Nikon Instruments, Inc.) on a Nikon Eclipse Ti-S microscope (Nikon Instruments, Inc.) at a frame rate of 3.37 frames per second.

Statistical analysis

All data shown represent experiments with at least $n=3$ individual microfluidic devices. Reported values correspond to averages over these devices for any given condition. Error bars were calculated using standard error. Significance was calculated using a two-tailed Student's t test and p-values are supplied in the Supplementary Tables S1–S6.

Results

Fibroblast stabilization

In initial experiments, we used a microfluidic device with a single gel region seeded with ECs alone (data not shown). ECs alone did form vascular networks after 2 days of culture. However, these networks subsequently regressed with time. It has been shown that coculture with fibroblasts enhances microvascular network formation in sprouting angiogenesis,[20,21] vasculogenesis,[10] and in mixed coculture experiments.[11] We suspected that fibroblasts in noncontact coculture might also be important in stabilizing the nascent vascular networks before they regress. Using the revised multiculture version of our microfluidic device to encapsulate fibroblasts in the adjacent gel regions, we indeed found that the presence of fibroblasts effectively stabilized the MVNs as measured by the total vascularized area and network perfusability (Fig. 2). In the case of monoculture, these properties gradually decreased after initial network formation, consistent with our preliminary experiments. However, under coculture conditions, they reached a stable plateau after 4 days.

Paracrine signaling

In an attempt to recapitulate the stabilizing effects of the fibroblasts, proangiogenic growth factors—VEGF (50 ng/mL) and S1P (250 nM)—were added to the growth medium. We chose these growth factors and specific concentrations based on previous work in our laboratory in which they

FIG. 2. **(A)** Phase contrast images (4×) of MVNs formed by endothelial cells (ECs) in isolated monoculture with EGM-2 MV medium (control) or in fibroblast coculture with EGM-2 MV medium. After day 4, control networks regress, while coculture networks remain intact. Scale bar = 1 mm. **(B)** Area covered by MVNs under monoculture and coculture conditions over a 6-day period. Values given are averages over at least three devices with error bars given as standard error (same for **C, D**). **(C)** Percentage of perfusable segments as defined by vascularized gel regions opening to medium channel containing at least one patent lumen. **(D)** Perfusable segments at day 6 as a function of fibroblast seeding density.
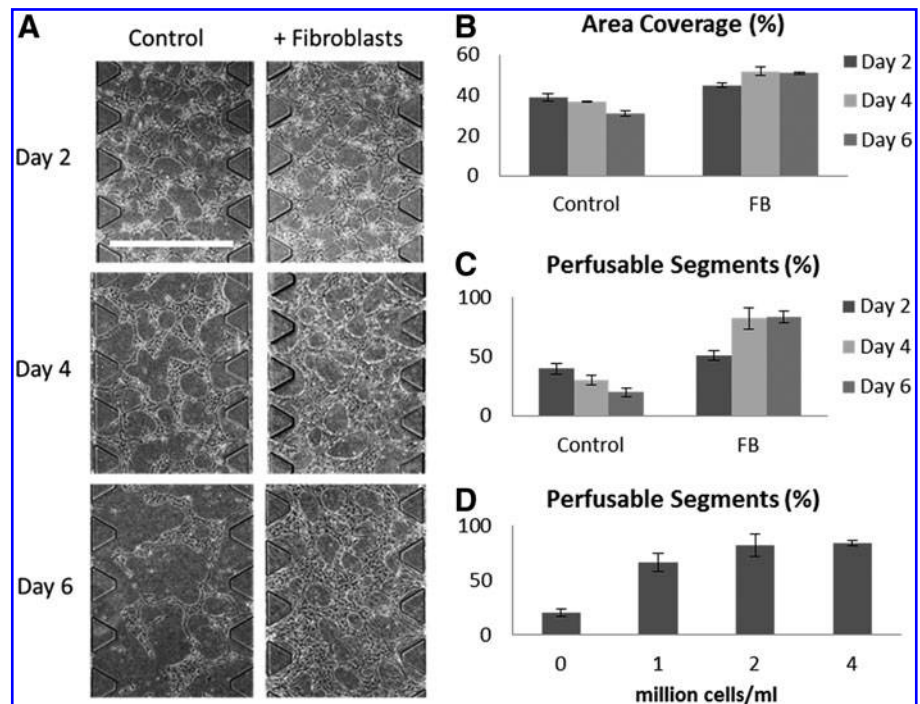
enhanced vessel sprouting and lumen formation in an angiogenesis model.[18] These growth factors did not significantly improve the long-term stability of the networks. However, they did give rise to vascular networks with significantly different morphological characteristics (Fig. 3). The resulting networks contained more branches with shorter average length and smaller diameters than those cultured with fibroblasts or alone in EGM-2 MV growth medium. The thinner structures in these networks covered less of the total area. Interestingly, by combining fibroblast coculture with the supplemented growth factors, we were able to achieve the larger coverage area and network stability provided by fibroblast coculture, while maintaining the reduced diameters and average length induced by the angiogenic growth factors.

Fibrin concentration

Fibrin gel was chosen for our experiments due to its biological relevance during tissue regrowth at wound healing sites and its unique mechanical properties. Specifically, fibrin gel demonstrates strain stiffening, which allows it to be easily deformed by network forming ECs at small strains, while maintaining its overall structural stability at the network level.[22] It is capable of undergoing large, recoverable deformations and can withstand considerably large strains

before rupture.[23–25] We chose to alter the mechanical properties of our fibrin gel by varying the fibrinogen concentration from 1.5 to 10 mg/mL. The fibrinogen concentration is a key determining factor of the mechanical structure and strength of fibrin gels and has been shown to influence MVN formation.[26,27] We found that the number of branches in a network was highly sensitive to the fibrinogen concentration, while the coverage area remained little changed over the entire range of concentrations studied. Both the average branch length and effective diameter decreased with increasing fibrinogen concentrations (Fig. 4). The change in effective diameter between the two extreme conditions was $17.1\% \pm 4.6\%$.
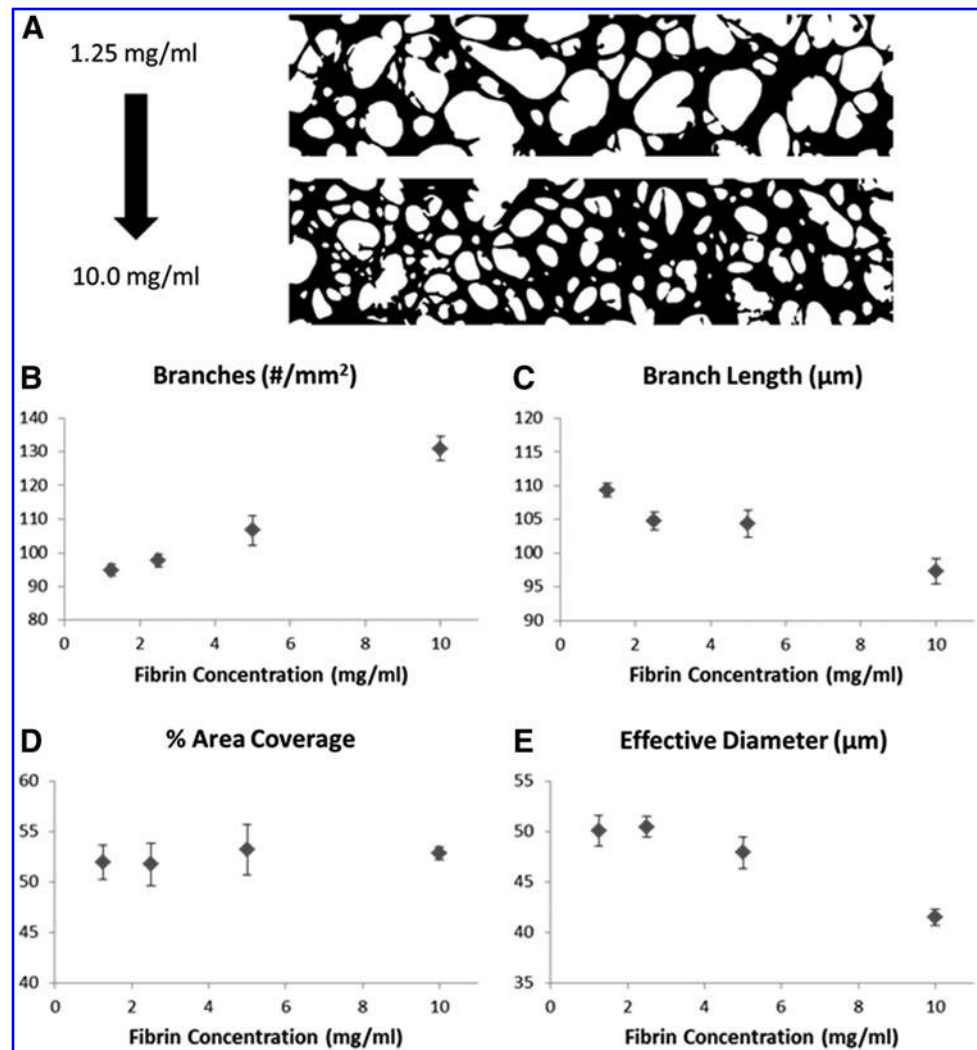
HUVEC seeding density

We found that HUVEC seeding density plays an important role in MVN formation and the resulting network morphology. At a HUVEC seeding density of one million cells/mL, we found that sparse networks formed with comparatively short branches and small diameters. This represents the lowest seeding density achievable, beyond which perfusable MVNs will not form. With increasing seeding density, we found that the branch length, diameter, and area fraction of the vascularized region all increased (Fig. 5).
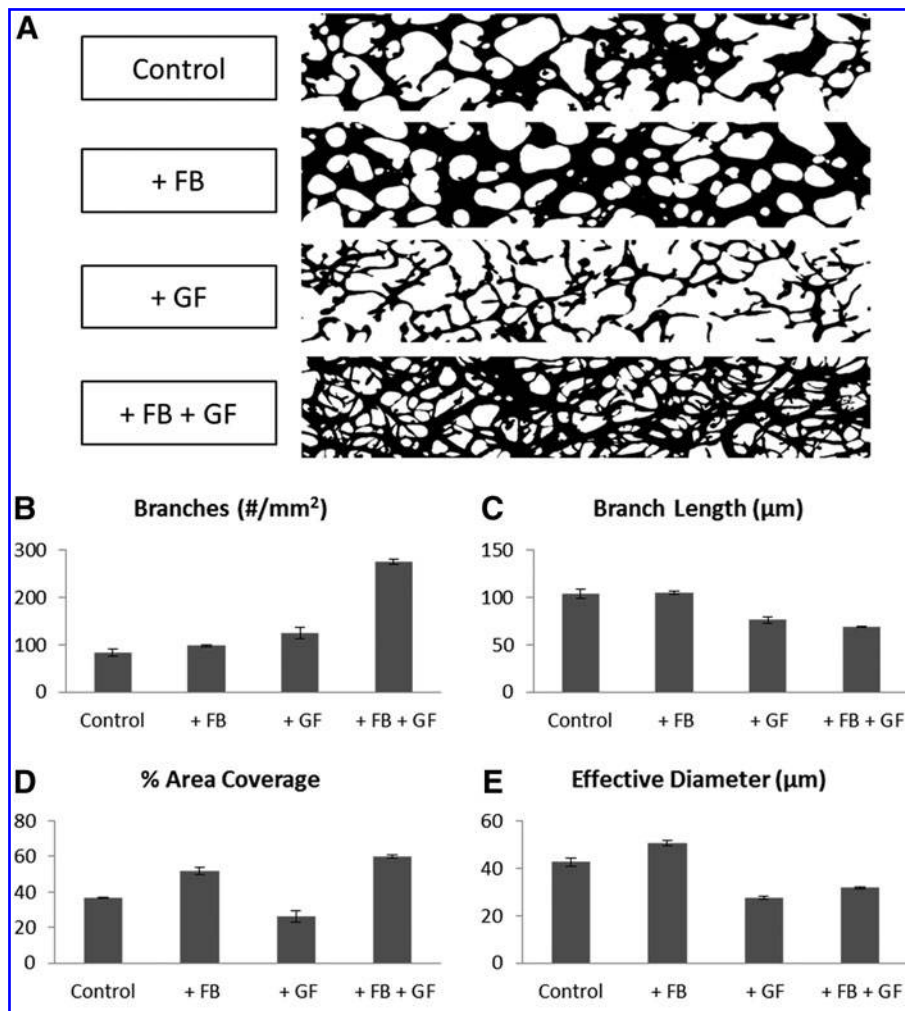
FIG. 3. (A) Representative binary images of MVNs formed under conditions of endothelial cell (EC) monoculture in EGM-2 MV medium; EC + Fibroblast (FB) noncontact coculture in EGM-2 MV medium; EC monoculture with EGM-2 MV medium supplemented with vascular endothelial growth factor (VEGF) (50 ng/mL) and sphingosine-1-phosphate (S1P) (250 nM); EC + FB noncontact coculture in EGM-2 MV medium supplemented with VEGF and S1P. Fixed networks were stained with phalloidin and ImageJ was used to process and binarize fluorescent images. One image from each condition was chosen arbitrarily to represent the group. (B) Number of branches per mm² of vascularized region. Values given are averages over three devices with error bars given as standard error (same for C–E). (C) Average branch length of MVN. (D) Percentage of area covered by perfusable MVN. (E) Effective diameter of vessels in engineered MVN, calculated as the ratio of vascularized area to total length of engineered MVN; GF, growth factor.

FIG. 4. (A) Representative binary images of MVNs formed under conditions of increasing fibrinogen concentration for fibrin gel cell encapsulation experiments. One image from each condition was chosen arbitrarily to represent the group. Fixed networks were stained with phalloidin; ImageJ was used to process and binarize fluorescent images. (B) Number of branches per mm^2 of vascularized region. Values given are averages over three to four devices with error bars given as standard error (same for C–E). (C) Average branch length of MVN. (D) Percentage of area covered by perfusable MVN. (E) Effective diameter of vessels in engineered MVN, calculated as the ratio of vascularized area to total length of engineered MVN.

Fibroblast seeding density

The fibroblasts in our system are physically separated from the HUVECs and their effect on MVN formation is through paracrine signaling. We tested to see whether the amount of fibroblasts cultured in the stromal cell gel region had a significant impact on the engineered MVN morphology. Holding the HUVEC seeding density constant at 4 million cells/mL, we varied the amount of fibroblasts seeded from one half to twice the amount of HUVECs seeded. We found no significant differences in any of the measured MVN parameters (data not shown). Interestingly, we found that the stabilizing effect—as measured by the percentage of perfusable segments at day 6—was dose dependent on the amount of fibroblasts present and reached a steady maximum value at a HUVEC:HLF ratio of 1:1 (Fig. 2C).

Discussion

The ultimate goal of tissue engineering is to replace ailing tissues and failing organs *in vivo*. It has been increasingly realized that forming prevascularized tissue *in vitro* may be a necessary first step.[15,28,29] Additionally, *in vitro* platforms enabling the growth and maintenance of a functional microvasculature provide significant benefits in their own right. Perfusable, *in vitro* models can be used as physiological

drug-screening platforms for developing and identifying metastasis preventing cancer drugs.[30,31] As demonstrated here, the system can be used to isolate the environmental factors influencing MVN formation and to study their effects. This is an important step in continuing to develop tissue engineering as a quantitative science and to enhance control in the design of tissue-engineered constructs. Whereas the present experiments have been performed in an *in vitro* system, not intended for *in vivo* use, we anticipate that the design principles we discovered would apply for other, similar tissue-engineered constructs. Alternatively, by nonpermanently sealing the device with a second layer of PDMS—rather than a glass coverslip—we can successfully remove the vascularized hydrogel after it forms. The removed constructs could potentially be implanted directly *in vivo*.

We successfully formed MVNs using our system containing vessels with diameters ranging between 1 and 100 µm. These vessels form complex, interconnected networks and are perfusable. It is known that the flow characteristics of blood perfusing through the vasculature is important in determining and maintaining network morphology. In one *in vitro* study, it was found that interstitial flow during vasculogenesis was necessary to form perfusable MVNs.[11] This was not the case for our system in which
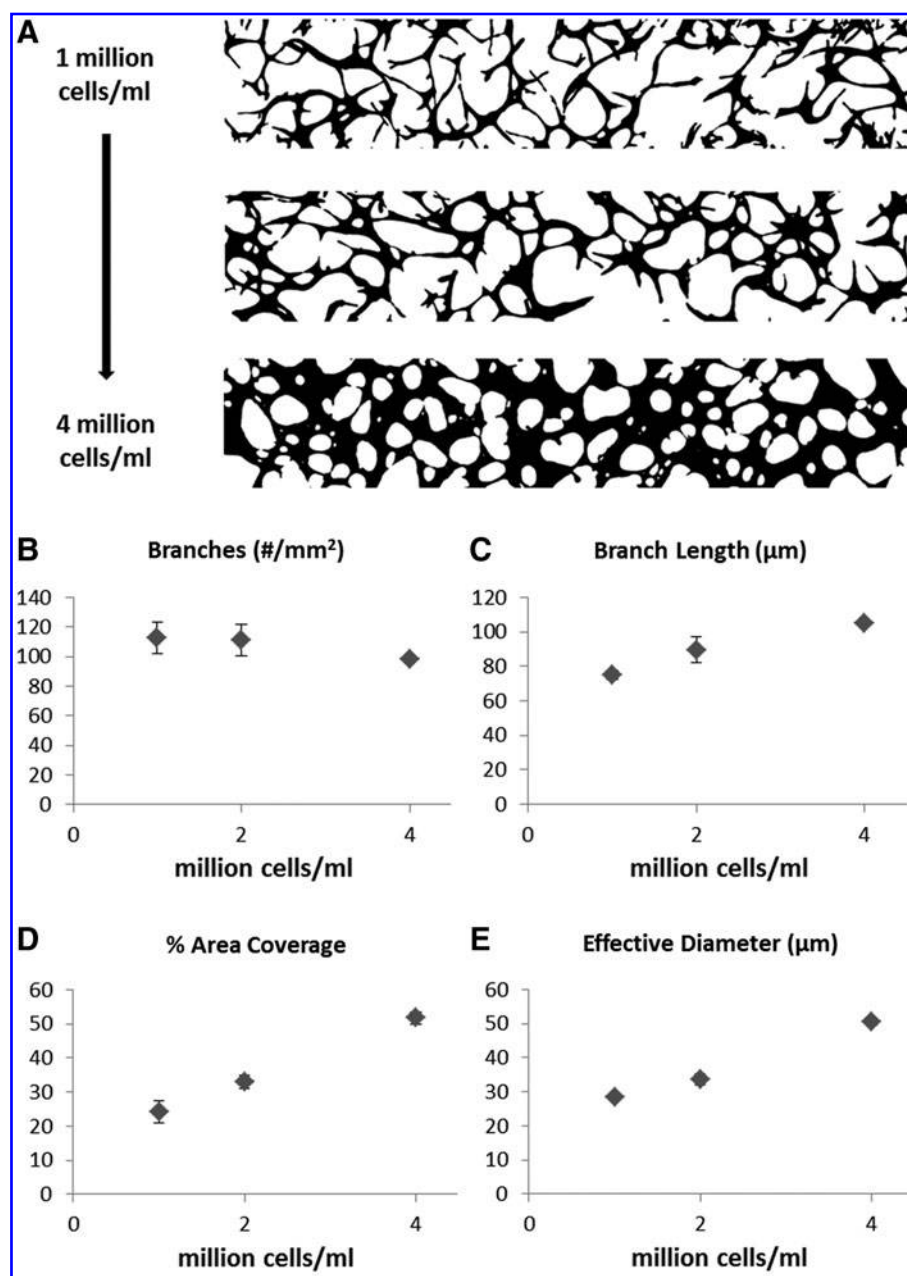
FIG. 5. **(A)** Representative binary images of MVNs formed under conditions of increasing human umbilical vein endothelial cell (HUVEC) seeding density. One image from each condition was chosen arbitrarily to represent the group. Fixed networks were stained with phalloidin and ImageJ was used to process and binarize fluorescent images. **(B)** Number of branches per mm² of vascularized region. Values given are averages over three devices with error bars given as standard error (same for **C–E**). **(C)** Average branch length of MVN. **(D)** Percentage of area covered by perfusable MVN. **(E)** Effective diameter of vessels in engineered MVN, calculated as the ratio of vascularized area to total length of engineered MVN.

perfusable networks formed in the absence of flow. However, it is plausible that interstitial flow might affect the dynamics of network formation and the resulting morphology. Interstitial flow has been shown to affect cancer cell migration[32] and angiogenic sprouting through an integrin-mediated sensing mechanism,[33] which may also be important during vasculogenic network formation. In this study, we focused on preflow factors and showed that they direct the early stages of MVN formation in vasculogenesis. In future studies, it will be interesting to study the relative importance of flow through the networks after initial formation as it is also likely to play an important role. Flow-induced shear stress sensed by the endothelium acts to regulate the diameter of blood vessels *in vivo*.[34] It also leads to the pruning of extraneous branches eventually directing the vascular network morphology toward an energetically optimal pattern.[35,36] We would expect that similar phenomena

would occur in our system with the addition of flow. This could be confirmed by introducing tracer particles into the networks to visualize the flow field and correlating regions of pruned vessels to regions of limited flow. The presence of chronic shear flow[36] and the introduction of stabilizing pericytes[37,38] would also provide a more authentically native microvascular environment and would likely lead to network morphologies that more closely mimic those found *in vivo*.

In designing vascularized tissue, it is important to consider that, *in vivo*, ECs form vascular networks within a complex environment involving dynamic heterotypical interactions. In addition to mechanical and signaling cues provided by the surrounding extracellular matrix, communication with supporting cell types is critical.[39,40] Our microfluidic system allows for spatial segregation of various cell types in a compact environment enabling communication through the diffusion
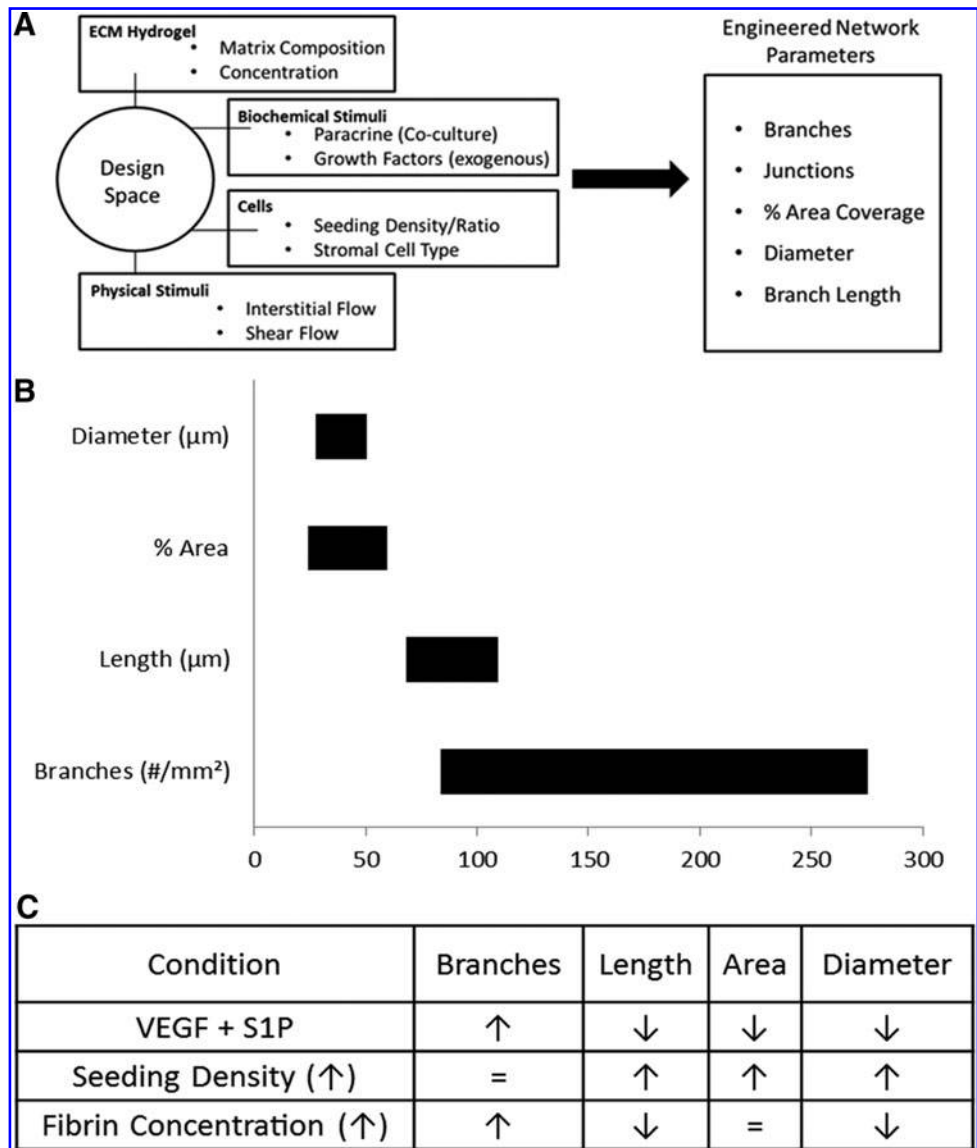
of soluble factors. By culturing the two cell types together in a single gel region, we could also study the potential stabilizing effects due to cell–cell contact and juxtacrine signaling between the two cell types and fibroblast remodeling of the ECM. It has been shown that the stabilizing effects of MSCs on MVN formation *in vitro* depend on the time at which MSCs are introduced into the mixed coculture system. Interestingly, MSCs only promoted network stability when introduced at least 24 h after EC seeding.[41] Seeding two cell types simultaneously in the same gel would presumably alter the chemical gradient profiles, lead to a competition for local nutrients and cytokines, and affect the structural properties of the ECM in which ECs are forming a vascular network.

The stabilizing effect of fibroblasts in our noncontact coculture system was striking. Without HLFs, the nascent EC networks quickly regressed after initial formation. However, through communication with HLFs, these nascent networks were able to maintain a stable morphology and level of perfusability. These results are in agreement with those found by Kim *et al.*,[10] in which a lumenized vasculature was lacking after 4 days of EC culture without fibroblasts present. Our results further elucidate that vascular networks do initially form, but subsequently regress in the absence of a second cell type. It has been shown that fibroblasts enhance MVN formation through direct paracrine signaling[20] and also by adapting the ECM through secreted molecules.[21] It will be interesting in future studies to observe the ECM in real time during MVN formation to characterize this process. It will also be useful to test the effects of various other stromal cells and determine their efficacy in MVN formation for use in regenerative cell therapies.

An important finding from our study is that factors secreted from fibroblasts affect the processes of (a) network formation and (b) stabilization independently. When HUVECs were cultured with HLFs alone, the networks formed with a larger diameter than the control condition and maintained perfusability through day 6. HUVECs cultured with VEGF and S1P formed networks with a smaller diameter and regressed with time. Combining HLF coculture with VEGF and S1P produced networks with smaller diameters

FIG. 6. **(A)** Diagram of design approach to microvascular tissue engineering. Use of microfluidic platform to quantify effects of mechanical and chemical stimuli on resulting network morphology. Novel, noncontact multiculture system to study cell–cell communication and network stabilization. **(B)** Range of network parameters achievable through control of inputs studied. **(C)** Table of the effects of tunable inputs on distinct network morphological parameters.

Condition	Branches	Length	Area	Diameter
VEGF + S1P	↑	↓	↓	↓
Seeding Density (↑)	=	↑	↑	↑
Fibrin Concentration (↑)	↑	↓	=	↓

that remained stable. This suggests that different growth factors might independently control the individual characteristics of network morphology and that this process is also independent of network stabilization. Future work will explore the individual effects of specific growth factors known to be involved in vasculogenesis.

We produced a table of results (Fig. 6), which captures our design approach to microvascular engineering and summarizes our findings. In this study, we mapped out the design space for the creation of MVNs with prescribed morphological properties. The controllable inputs we studied were cell seeding densities, ECM composition, and paracrine signaling factors. The output metrics we analyzed were the number of branches, average branch length, area fraction of vascularization, and effective diameter. These properties proved sufficient to quantitatively describe the significant differences in network morphology observed by varying environmental conditions. The list of environmental factors studied here is not exhaustive, and future work will utilize this system and approach to expand in both breadth and depth. Additionally, to further probe the mechanisms underlying the observations found in this study, it would be useful to pair these experiments with a computational modeling approach.[42–44] In closing, this study provides a significant contribution to the effort of quantifying the science of microvascular tissue engineering and creating MVNs with prescribed morphological properties for tissue-specific applications.

Acknowledgments

Disclosure Statement

The authors wish to disclose that RDK has financial interests in a company, AIM Biotech, which develops microfluidic systems of the type used in this study.

References

1. Kassab, G.S. Scaling laws of vascular trees: of form and function. Am J Physiol Heart Circ Physiol **290,** H894, 2006.
2. Muschler, G.F., Nakamoto, C., and Griffith, L.G. Engineering Principles of Clinical Cell-Based Tissue Engineering. J Bone Jt Surg **86,** 1541, 2004.
3. Hoganson, D.M. *et al.* Principles of Biomimetic Vascular Network Design Applied to a Tissue-Engineered Liver Scaffold. Tissue Eng Part A **16,** 1469, 2010.
4. Murray, C.D. The Physiological Principle of Minimum Work I. The Vascular System and the Cost of Blood Volume. Proc Natl Acad Sci **12,** 207, 1926.
5. Barber, R.W., and Emerson, D.R. Biomimetic design of artificial micro-vasculatures for tissue engineering. Altern Lab Anim ATLA **38 Suppl 1,** 67, 2010.
6. Okkels, F., and Jacobsen, J.C.B. Dynamic adaption of vascular morphology. Front Fractal Physiol **3,** 390, 2012.
7. Pries, A.R., Secomb, T.W., and Gaehtgens, P. Design Principles of Vascular Beds. Circ Res **77,** 1017, 1995.
8. Borenstein, J.T., *et al.* Functional endothelialized microvascular networks with circular cross-sections in a tissue culture substrate. Biomed Microdevices **12,** 71, 2010.

9. Chrobak, K.M., Potter, D.R., and Tien, J. Formation of perfused, functional microvascular tubes *in vitro*. Microvasc Res **71,** 185, 2006.
10. Kim, S., Lee, H., Chung, M., and Jeon, N.L. Engineering of functional, perfusable 3D microvascular networks on a chip. Lab Chip **13,** 1489, 2013.
11. Moya, M.L., Hsu, Y.-H., Lee, A.P., Hughes, C.C.W., and George, S.C. In Vitro Perfused Human Capillary Networks. Tissue Eng Part C Methods **19,** 730, 2013.
12. Chan, J.M., *et al.* Engineering of In Vitro 3D Capillary Beds by Self-Directed Angiogenic Sprouting. PLoS One **7,** e50582, 2012.
13. Shin, Y., *et al.* Microfluidic assay for simultaneous culture of multiple cell types on surfaces or within hydrogels. Nat Protoc **7,** 1247, 2012.
14. Chung, S., *et al.* Cell migration into scaffolds under co-culture conditions in a microfluidic platform. Lab Chip **9,** 269, 2009.
15. Kaully, T., Kaufman-Francis, K., Lesman, A., and Levenberg, S. Vascularization—the conduit to viable engineered tissues. Tissue Eng Part B Rev **15,** 159, 2009.
16. Chen, X., *et al.* Prevascularization of a fibrin-based tissue construct accelerates the formation of functional anastomosis with host vasculature. Tissue Eng Part A **15,** 1363, 2009.
17. Tonello, C., *et al. In vitro* reconstruction of human dermal equivalent enriched with endothelial cells. Biomaterials **24,** 1205, 2003.
18. Lim, S.H., Kim, C., Aref, A.R., Kamm, R.D., and Raghunath, M. Complementary effects of prolyl hydroxylase inhibitors and sphingosine 1-phosphate on fibroblasts and endothelial cells in driving capillary sprouting Integer Biol (Camb) **5,** 1474, 2013.
19. Arganda-Carreras, I., Fernández-González, R., Muñoz-Barrutia, A., and Ortiz-De-Solorzano, C. 3D reconstruction of histological sections: application to mammary gland tissue. Microsc Res Tech **73,** 1019, 2010.
20. Nakatsu, M.N., *et al.* Angiogenic sprouting and capillary lumen formation modeled by human umbilical vein endothelial cells (HUVEC) in fibrin gels: the role of fibroblasts and Angiopoietin-1☆. Microvasc Res **66,** 102, 2003.
21. Newman, A.C., Nakatsu, M.N., Chou, W., Gershon, P.D., and Hughes, C.C.W. The requirement for fibroblasts in angiogenesis: fibroblast-derived matrix proteins are essential for endothelial cell lumen formation. Mol Biol Cell **22,** 3791, 2011.
22. Janmey, P.A., Winer, J.P., and Weisel, J.W. Fibrin gels and their clinical and bioengineering applications. J R Soc Interface **6,** 1, 2009.
23. Piechocka, I.K., Bacabac, R.G., Potters, M., MacKintosh, F.C., and Koenderink, G.H. Structural Hierarchy Governs Fibrin Gel Mechanics. Biophys J **98,** 2281, 2010.
24. Brown, A.E.X., Litvinov, R.I., Discher, D.E., Purohit, P.K., and Weisel, J.W. Multiscale Mechanics of Fibrin Polymer: Gel Stretching with Protein Unfolding and Loss of Water. Science **325,** 741, 2009.
25. Liu, W., *et al.* Fibrin fibers have extraordinary extensibility and elasticity. Science **313,** 634, 2006.
26. Ryan, E., Mockros, L., Weisel, J., and Lorand, L. Structural origins of fibrin clot rheology. Biophys J **77,** 2813, 1999.
27. Ghajar, C.M., *et al.* The effect of matrix density on the regulation of 3-d capillary morphogenesis. Biophys J **94,** 1930, 2008.
28. Gibot, L., Galbraith, T., Huot, J., and Auger, F.A. A preexisting microvascular network benefits *in vivo* revascularization of a microvascularized tissue-engineered skin substitute. Tissue Eng Part A **16,** 3199, 2010.

29. Laschke, M.W., *et al.* Angiogenesis in tissue engineering: breathing life into constructed tissue substitutes. Tissue Eng **12,** 2093, 2006.

30. Ghaemmaghami, A.M., Hancock, M.J., Harrington, H., Kaji, H., and Khademhosseini, A. Biomimetic tissues on a chip for drug discovery. Drug Discov Today **17,** 173, 2012.

31. Chen, M.B., Whisler, J.A., Jeon, J.S., and Kamm, R.D. Mechanisms of tumor cell extravasation in an *in vitro* microvascular network platform. Integr Biol **5,** 1262, 2013.

32. Polacheck, W.J., Charest, J.L., and Kamm, R.D. Interstitial flow influences direction of tumor cell migration through competing mechanisms. Proc Natl Acad Sci U S A **108,** 11115, 2011.

33. Vickerman, V., and Kamm, R.D. Mechanism of a flow-gated angiogenesis switch: early signaling events at cell–matrix and cell–cell junctions. Integr Biol **4,** 863, 2012.

34. Udan, R.S., Vadakkan, T.J., and Dickinson, M.E. Dynamic responses of endothelial cells to changes in blood flow during vascular remodeling of the mouse yolk sac. Development **140,** 4041, 2013.

35. Kochhan, E., *et al.* Blood flow changes coincide with cellular rearrangements during blood vessel pruning in zebrafish embryos. PLoS One **8,** e75060, 2013.

36. Skalak, T.C., and Price, R.J. The role of mechanical stresses in microvascular remodeling. Microcirculation **3,** 143, 1996.

37. Von Tell, D., Armulik, A., and Betsholtz, C. Pericytes and vascular stability. Exp Cell Res **312,** 623, 2006.

38. Armulik, A., Abramsson, A., and Betsholtz, C. Endothelial/pericyte interactions. Circ Res **97,** 512, 2005.

39. Gaengel, K., Genové, G., Armulik, A., and Betsholtz, C. Endothelial-mural cell signaling in vascular development and angiogenesis. Arterioscler Thromb Vasc Biol **29,** 630, 2009.

40. Darland, D.C., and D'Amore, P.A. Cell-cell interactions in vascular development. Curr Top Dev Biol **52,** 107, 2001.

41. Duffy, G.P., Ahsan, T., O'Brien, T., Barry, F., and Nerem, R.M. Bone marrow-derived mesenchymal stem cells promote angiogenic processes in a time- and dose-dependent manner *in vitro*. Tissue Eng Part A **15,** 2459, 2009.

42. Merks, R.M.H., Brodsky, S.V., Goligorksy, M.S., Newman, S.A., and Glazier, J.A. Cell elongation is key to *in silico* replication of *in vitro* vasculogenesis and subsequent remodeling. Dev Biol **289,** 44, 2006.

43. Czirok, A., and Little, C.D. Pattern formation during vasculogenesis. Birth Defects Res Part C Embryo Today Rev **96,** 153, 2012.

44. Merks, R.M.H., and Koolwijk, P. Modeling morphogenesis *in silico* and *in vitro*: towards quantitative, predictive, cell-based modeling. Math Model Nat Phenom **4,** 149, 2009.

Address correspondence to:
Roger D. Kamm, PhD
Department of Biological Engineering
Massachusetts Institute of Technology
500 Technology Square
MIT Building NE47 Room 321
Cambridge, MA 02139

E-mail: rdkamm@mit.edu

This article has been cited by:

1. David G. Belair, Jordan A. Whisler, Jorge Valdez, Jeremy Velazquez, James A. Molenda, Vernella Vickerman, Rachel Lewis, Christine Daigh, Tyler D. Hansen, David A. Mann, James A. Thomson, Linda G. Griffith, Roger D. Kamm, Michael P. Schwartz, William L. Murphy. 2015. Human Vascular Tissue Models Formed from Human Induced Pluripotent Stem Cell Derived Endothelial Cells. *Stem Cell Reviews and Reports* **11**, 511-525. [CrossRef]

2. Bichsel Colette A., Hall Sean R.R., Schmid Ralph A., Guenat Olivier T., Geiser Thomas. Primary Human Lung Pericytes Support and Stabilize In Vitro Perfusable Microvessels. *Tissue Engineering Part A*, ahead of print. [Abstract] [Full Text HTML] [Full Text PDF] [Full Text PDF with Links] [Supplemental Material]

3. Simone Bersini, Matteo Moretti. 2015. 3D functional and perfusable microvascular networks for organotypic microfluidic models. *Journal of Materials Science: Materials in Medicine* **26**. . [CrossRef]

4. Miss Colette A. Bichsel, Dr. Sean R. R. Hall, Dr. Ralph A. Schmid, Dr. Olivier Guenat, Prof. Thomas Geiser. Primary human lung pericytes support and stabilize <i>in vitro</i> perfusable microvessels. *Tissue Engineering Part A* **0**:ja. . [Abstract] [Full Text PDF] [Full Text PDF with Links]

5. Sebastien G.M. Uzel, Andrea Pavesi, Roger D. Kamm. 2014. Microfabrication and microfluidics for muscle tissue models. *Progress in Biophysics and Molecular Biology* . [CrossRef]

6. Jessie S. Jeon, Simone Bersini, Jordan A. Whisler, Michelle B. Chen, Gabriele Dubini, Joseph L. Charest, Matteo Moretti, Roger D. Kamm. 2014. Generation of 3D functional microvascular networks with human mesenchymal stem cells in microfluidic systems. *Integr. Biol.* **6**, 555-563. [CrossRef]

7. Harry Z. An, H. Burak Eral, Lynna Chen, Michelle B. Chen, Patrick S. Doyle. 2014. Synthesis of colloidal microgels using oxygen-controlled flow lithography. *Soft Matter* **10**, 7595-7605. [CrossRef]